COMPARING OF CFD CONTOURS USING IMAGE ANALYSING METHOD: A STUDY ON VELOCITY DISTRIBUTIONS

Ahmet ERDOĞAN[1,2]*, Mahmut DAŞKIN[1,3]

[1]*İnönü University, Faculty of Engineering, Department of Mechanical Engineering, 44280, Malatya, Türkiye*
[2]*University of Nottingham, Faculty of Engineering, Advanced Materials Research Group, NG72RD, Nottingham, UK*
[3]*Cranfield University, Energy and Sustainability Theme, MK43 0AL, Cranfield, UK*

Abstract: Contour plotting, a widely utilized graphical technique for visualizing CFD (Computational Fluid Dynamics) outcomes, is highly valuable. It provides an effective and practical approach to analysing distributions of magnitudes belonging to fluid domains such as; velocity, temperature, pressure, volume fraction, etc. Nevertheless, when analysing multiple contours, especially showing similar distribution, identifying the ideal contour can be difficult and open to speculation. In this research, the issue was addressed by employing the Image Analysis Method for the classification of velocity distribution contours. This led to determining which picture has the best distribution among a few of the contour's pictures. Firstly, velocity distribution contours downstream of the diffuser located in Air Handling Unit (AHU) unit were obtained by using CFD. The contour pictures were then transferred to MATLAB environment. With pixel analysis in MATLAB, the pictures were able to be classified based on which parameters had an effect on the velocity distribution. Variable parameters are the length of the fan channel (x) and the ratio of cross-sectional areas of the AHU (A/A_o). The results showed that $x=250$ mm and $A/A_o=0.5$ improved velocity distributions by 6% and 20%, respectively.

Keywords: Computational fluid dynamics, Image analysis method, Velocity distribution, Air handling unit

1. Introduction

Fluid flow problems are numerically solved using the principles of conservation of mass, momentum, and energy, also known as computational fluid dynamics (CFD) (Hu, 2012). The characteristics of fluid domains can be determined with CFD by revealing magnitudes belonging to the fluid domain such as; the velocity, pressure, shear stress, temperature, turbulence, and volume fraction (Anderson and Wendt, 1995; Versteeg and Malalasekera, 2007). CFD results can be visualized via contour plots, which provide valuable and useful graphical tools (Tu et al., 2023). It always challenging to find the optimal contour plot when comparing multiple contour plots with similar distributions. Interpreting CFD contour plots that show similar distributions to each other without subjecting them to a numerical analysis and deciding which one gives better results may vary from person to person and may lead to erroneous interpretations and decisions. To classify the CFD results, which are presented as contour plots showing the velocity distribution of airflows, this study includes a series of CFD simulations based on airflow in air handling units (AHUs).

Air handling units serve as part of ventilation, heating, and air conditioning systems (HVAC) to regulate and circulate air (Parsons, 1996; Xu et al., 1996). In many applications of AHU, perforated diffusers are used to diffuse as homogeneously as possible the air supplied by the fan (Kamer et al., 2018). Otherwise, the air cannot entirely be in contact with the other units such as serpentines or humidifiers and AHUs may inefficiently work (Bayramgil et al., 1998). The pressure loss caused by perforated diffusers and velocity distributions downstream of them are two performance characteristics. The performance characteristics of V profile diffusers (Kamer et al., 2018), truncated pyramid diffusers (Bulut et al., 2011; Erdoğan, 2017), truncated cone diffusers (Sönmez, 2017), anemostat type diffusers (Vakkasoglu et al., 2021), and plate diffusers (Kerim Sönmez and Özmen, 2022) have been numerically studied. As with perforated diffusers, perforated plates are frequently used to manage flow in flow systems (Gan and Riffat, 1997; Özahi, 2015). Some researchers have reported the pressure losses and velocity distributions of perforated diffusers (Gaulke and Dreyer, 2015; Guo et al., 2013; Wang et al., 2020). In these studies, however, velocity distribution contours were interpreted without any image process which could assess the pictures. This might lead to a mistake in interpretation when contours showing small differences are considered.

Image analysing and image processes have been currently widely used in the assessment of CFD results of

different applications such as solar dryers (Benhamza et al., 2021), bubbles characteristics in the fluidised beds (Li et al., 2019), wind effect around buildings (He et al., 2021), and so on.

In this study, flow analyses were conducted using the Computational Fluid Dynamics (CFD) method considering two different geometric parameters, which have not been considered before, for a truncated pyramid perforated diffuser. The parameters considered were the length of fan channel (x) and the ratio of cross-sectional areas of the AHU (A/A_o). Velocity contours at the downstream region of the diffusers were obtained as a result of the CFD analysis with the grayscale contours colormap option. In this study, an initiative was taken to obtain parameter values resulting in optimal velocity distribution by transferring velocity contours to MATLAB software and analysing them using image matrices, rather than visually interpreting velocity contours.

2. Materials and Methods

In order to perform three-dimensional CFD analysis, solid models were firstly prepared and then transferred to the Ansys Fluent commercial software. Figure 1 depicts the solid model prepared for CFD analysis. In Figure 2, an AHU with diffuser is schematically shown with its dimensions and details.

In the prepared model, air enters uniformly through inlet section that has A of cross-sectional area. This inlet section was identified "velocity inlet" boundary condition. Upon reaching the sudden expansion region, a portion of the air collides with the truncated pyramid perforated diffuser through its holes, while the remaining portion bypasses the diffuser and exits the flow domain through an *800x800 mm* outlet section which was defined as "pressure outlet" boundary condition. All other boundaries were acknowledged as "wall" boundary conditioning with no slip condition. The height between the ceiling and the base of the square truncated pyramid perforated diffuser is 180 mm, with a thickness of 2 mm. Each face of the diffuser contains 45 holes. In Figure 2, x represents the length of the air supply channel, which is the first parameter. 100 mm, 150 mm, 200 mm, and 250 mm are the values in this study for x. Another parameter examined for its effect on diffuser velocity distributions is the ratio of cross-sectional areas of the AHU, symbolized by A/A_0. For four different values (0.2, 0.3, 0.4, and 0.5) of A/A_0, this parameter was considered to obtain velocity distribution contours at the downstream of the diffuser.
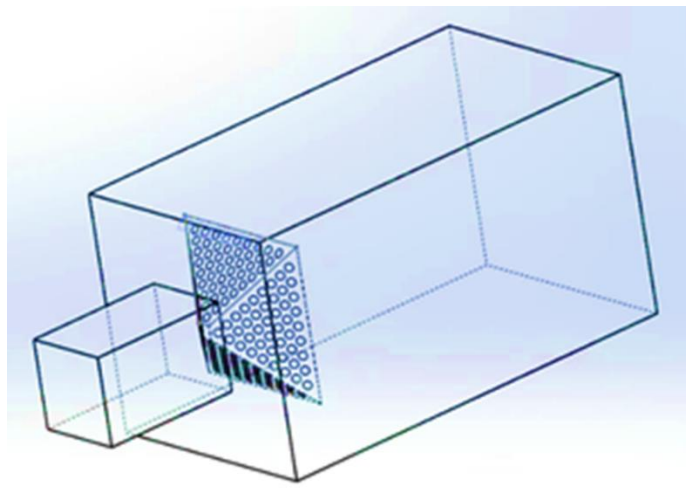

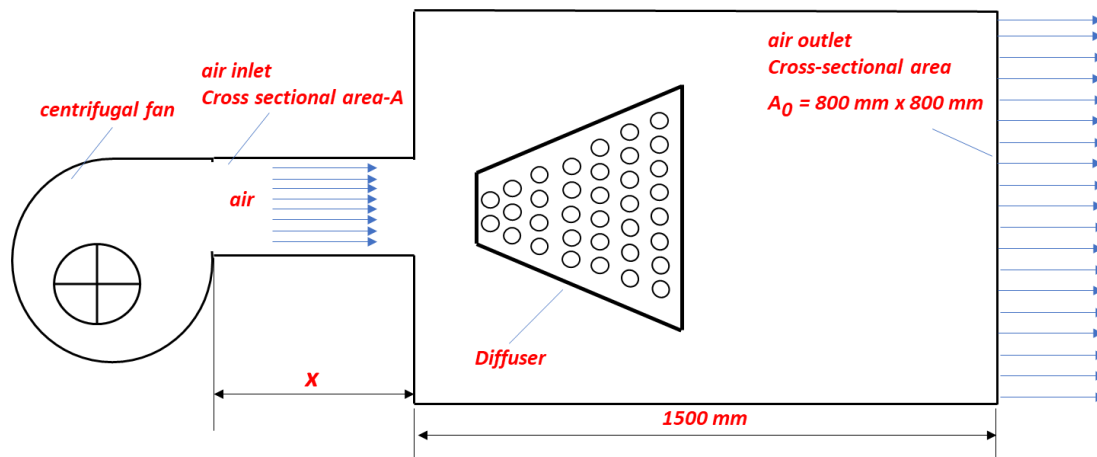**Figure 1.** Solid model prepared for CFD.

Figure 2. The dimensions and details of an AHU with diffusers.

In the models generated to perform CFD analyses, the mesh number is maintained at approximately $2.5*10^6$. There was no significant difference in the results when the mesh number is increased or decreased by 50%. A tetrahedral mesh type was defined for the entire flow domain. A dense mesh structure was created on the diffuser surfaces and hole sections, with a mesh size of 3 mm on the diffuser surface and a maximum size of 15 mm throughout the entire flow volume. The maximum skewness value all the meshes was preserved at 0.84. The mesh was refined in all of flow domain. 18° is determined for the span angle of the mesh curvature. Fine and high options are selected as the relevance centre and mesh smoothing characteristics. The turbulence intensity at the inlet was set to 5%, and the hydraulic diameter was set to 0.3 m. The entire flow domain was analysed under steady flow conditions. A pressure-based solver with the SIMPLE algorithm was used for the resolution of all models. This model was discretized spatially using the First Order Upwind Scheme as a method of spatial discretization. A convergence criterion of 10^{-3} was applied to all variables. Parallel processing was carried out on 8 processors for each analysis. The principles of conservation of mass, momentum, and additional motion equations were applied to the flow domain using the Finite Volume Method. The RANS (Reynolds Averaging Navier-Stokes) governing equations of mass and momentum are solved in CFD analyses. The governing Equations 1 and 2:

$$\frac{\partial u_i}{\partial x_i} = 0 \tag{1}$$

$$\frac{\partial u_i u_j}{\partial x_j} = -\frac{\partial p}{\partial x_i} + \frac{\partial}{\partial x_j}\left[\mu\left(\frac{\partial u_i}{\partial x_j} + \frac{\partial u_j}{\partial x_i}\right)\right] - \frac{\partial}{\partial x_j}(\rho \overline{u_i' u_j'}) \tag{2}$$

where u and p are the velocity and pressure, respectively.

$\overline{u_i' u_j'}$ states Reynolds stress. Since giving a good agreement between numerical simulations and experimental measurements in the flow analysis within AHUs (Kamer et al., 2018; Vakkasoglu et al., 2021), the CFD analyses were solved using the Standard k-ε turbulence model. The equations of Standard k-ε turbulence model are given Equation 3 and equation 4 (Chen and Kim, 1987).

$$\frac{\partial(\rho k)}{\partial t} + \frac{\partial(\rho k u_i)}{\partial x_i} = \frac{\partial}{\partial x_j}\left[\left(\mu + \frac{\mu_t}{\sigma_k}\right)\frac{\partial k}{\partial x_j}\right] + G_k - \rho\varepsilon \tag{3}$$

$$\frac{\partial(\rho\varepsilon)}{\partial t} + \frac{\partial(\rho\varepsilon u_i)}{\partial x_i} = \frac{\partial}{\partial x_j}\left[\left(\mu + \frac{\mu_t}{\sigma_\varepsilon}\right)\frac{\partial\varepsilon}{\partial x_j}\right] + C_{1\varepsilon}\frac{\varepsilon}{k}G_K - C_{2\varepsilon}\rho\frac{\varepsilon^2}{k} \tag{4}$$

In equation 3 and equation 4, turbulence kinetic energy and turbulence dissipation rate are symbolised k and ε, respectively. μ_t states turbulent viscosity and calculated equation 5 illustrated below.

$$\mu_t = \rho C_\mu \frac{k^2}{\varepsilon} \tag{5}$$

The constants in these equations take the following values, respectively: σ_k=1, σ_ε=1.3, $C_{1\varepsilon}$=1.44, $C_{2\varepsilon}$=1.92, and C_μ=0.09 (Fluent, 2009).

Velocity contours at the reference section downstream of the diffuser were obtained using the Ansys Fluent program. These velocity contours were transferred to the MATLAB environment as grayscale contours starting from black and ending with white. Investigation of these images was conducted in two stages using MATLAB program. Firstly, the pixel value corresponding to average velocity, which is desirable to have a velocity close to this level at every point on the cross-sectional area for a homogeneous velocity distribution, the value at the reference section downstream of the diffuser was determined. This process is illustrated in Figure 3.
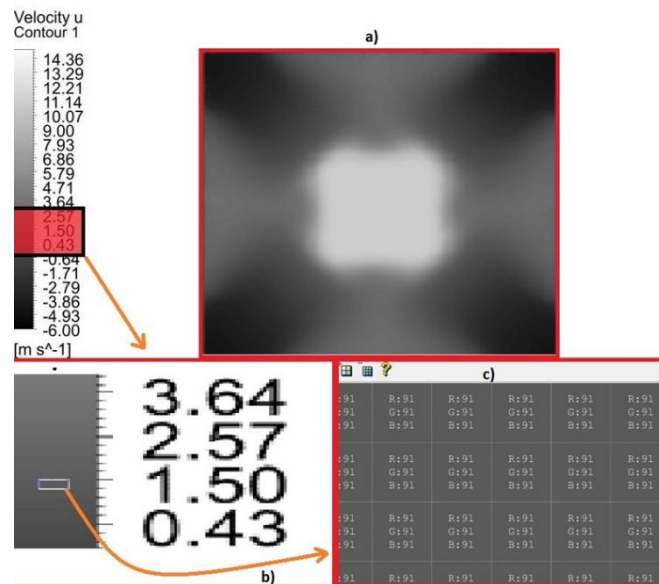

Figure 3. a) The velocity distribution contours obtained from CFD analysis. b) The region of interest where the average velocity is located. c) The image pixel values corresponding to the average velocity.

Secondly, the absolute difference between the pixel value corresponding to the average velocity and the matrix values of the respective velocity distribution images is obtained using the equation 6. This process yields an error value. This error computation was conducted across all pixels within the image, resulting in a comprehensive assessment of how closely the actual velocity distribution matched the desired average velocity. To facilitate a more meaningful comparison among different velocity distribution images, the obtained error values were normalized within the range of [0-1]. Normalization allowed for a consistent and fair evaluation of the images, regardless of their original scale or magnitude. Finally, the images were sorted based on their error values, providing a systematic way to identify and rank the performance of various diffuser configurations (Equation 6).

$$E = \sum_{x=1}^{n}\sum_{y=1}^{n}\left|\grave{I} - I_{xy}\right| \qquad (6)$$

Here, E is the error, $\grave{I}$ represents the pixel value corresponding to the average velocity, and I_{xy} states each pixel value associated with the image.

3. Results and Discussion

In this study, the velocity distribution characteristics of truncated pyramid perforated diffusers were examined. Velocity contours were obtained for a reference section located 400 mm horizontally from the sudden expansion section downstream of the diffuser using the ANSYS Fluent software package in the CFD analysis. Velocity distribution contours at the reference section for four different values of the length of the air supply channel ($x_1=100$ mm, $x_2=150$ mm, $x_3=200$ mm, and $x_4=250$ mm) are presented in Figure 4. Additionally, velocity contours obtained for the reference section in the downstream of the diffuser are provided in Figure 5 for four different values of the ratio of cross-sectional areas of the AHU ($A/A_0=0.2$, $A/A_0=0.3$, $A/A_0=0.4$, and $A/A_0=0.5$). It is obvious from Figures 4 and 5 that all pictures showing velocity distributions are not homogeneous. Moreover, Figure 4 illustrates the main objective of this study because the images showing velocity distribution are considerably close to each other.

In the studies where the performances of diffusers of different geometries used in AHUs were investigated by CFD, the images demonstrating contour plots were tried to be interpreted without any numerical analysis (A Erdoğan, 2016; Kamer et al., 2018; Vakkasoglu et al., 2021). In contrast, in this study, images displaying contour plots were analysed and classified using image analysis. By applying equation 6, the pixel values of the velocity contours for different lengths of the air supply channel values were analysed, and the normalized error values obtained from the analysis are presented in Table 1. As can be seen in Table 1, the length of air supply channel providing more homogeneous airflow

distribution in the reference section is $x_2=250$ mm since it has the minimum value among these normalized error values calculated for different lengths of air supply channel. At this point, as the air supply channel length increases, the airflow reaches the fully-developed turbulence flow profile (Gessner & Jones, 1965; Hussain & Reynolds, 1975) and may therefore result in improved diffuser performance.
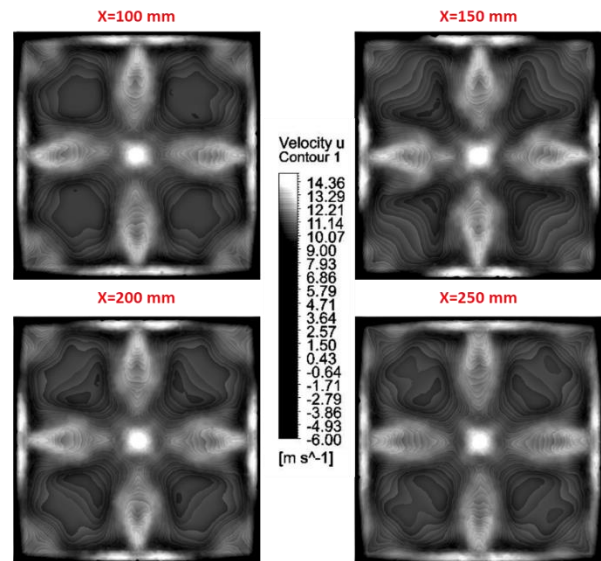

Figure 4. Velocity distribution contours obtained by CFD for the length of the air supply channel.
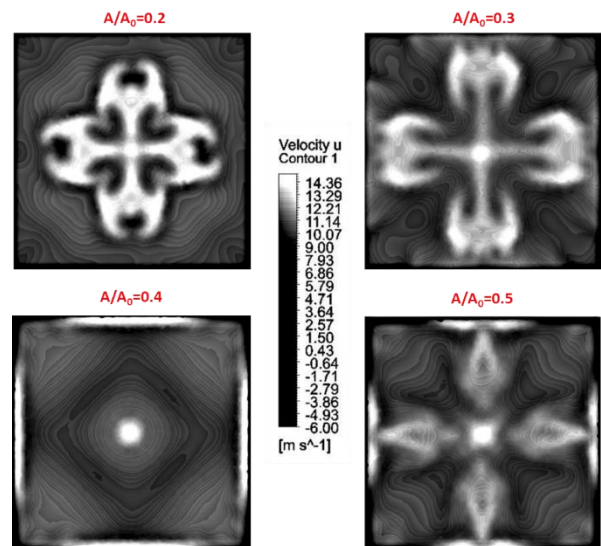

Figure 5. Velocity distribution contours obtained by CFD for the ratio of cross-sectional areas of the AHU.

Table 1. Normalised pixel errors values of the contours obtained for different lengths of the air supply channel

Parameter and values	Error
$x_1=100$ mm	1.0000
$x_2=150$ mm	0.9880
$x_3=200$ mm	0.9715
$x_4=250$ mm	0.9418

Table 2 gives normalized pixel error values of the contours obtained for different ratios of cross-sectional areas of the AHU. According to Table 2, the parameter value of $A/A_0 = 0.5$ is closest to the average velocity value corresponding to the reference cross-section highlighted in red in Figure 3 in terms of pixel value on the image. This shows that the diffuser with a ratio of cross-sectional areas of the AHU of $A/A_0 = 0.5$ possesses a lower error value and demonstrates superior distribution performance compared to other ratios of cross-sectional areas of the AHU.

Table 2. Normalised pixel error values of the contours obtained for different ratio of cross-sectional areas of the AHU

Parameter and values	Error
$A/A_0 = 0.2$	1.0000
$A/A_0 = 0.3$	0.9919
$A/A_0 = 0.4$	0.9321
$A/A_0 = 0.5$	0.8012

4. Conclusion

This study has focused on analysing velocity distribution contours using image analysis techniques to provide a numerical interpretation of computational fluid dynamics (CFD) contours, which are commonly presented in various CFD studies. To carry out this novelty, a few CFD simulations were conducted in AHU which has a diffuser. Velocity distribution contours at the reference cross-section downstream of the diffuser were obtained for two different parameters in the grayscale contour. Error values are calculated for each velocity contour to quantify the deviation from the contour representing the optimal velocity distribution. Within the scope of this study,

- It has been established that CFD outputs such as contour plots, which are often challenging to interpret or subject to debate, can be effectively interpreted using numerical image analysis techniques.
- Based on the image analysis, it appears that the minimum pixel error is reached if the length of air supply channel (x) is kept at 250 mm, and the velocity distribution could be improved by approximately 20%.
- In these ranges of parameters values, the pixel error obtained by the image analysis method can be minimised within these parameter scales if the ratio of AHU cross-sectional area (A/A_0) is 0.5. The velocity distribution is able to be developed by around 6% if the ratio of AHU cross-sectional area is 0.5.

In future studies, it is planned that this optimisation method could be applied to other CFD contours presenting such as temperature distribution, pressure distribution, and volume fraction of the fluid domain.

Author Contributions

The percentage of the author(s) contributions is presented below. All authors reviewed and approved the final version of the manuscript.

	A.E.	M.D.
C	50	50
D	50	50
S	60	40
DCP	80	20
DAI	20	80
L	60	40
W	50	50
CR	50	50
SR	50	50
PM	50	50

C=Concept, D= design, S= supervision, DCP= data collection and/or processing, DAI= data analysis and/or interpretation, L= literature search, W= writing, CR= critical review, SR= submission and revision, PM= project management.

Conflict of Interest

The authors declared that there is no conflict of interest.

Ethical Consideration

Ethics committee approval was not required for this study because of there was no study on animals or humans.

References

Anderson JD, Wendt J. 1995. Computational fluid dynamics. Springer, Berlin, Germany, pp: 3-14.

Bayramgil V, Bayrak S, Yükselen M, Erim M. 1998. Experimental investigation of a diffuser for cooling and air conditioning system. 21st Congress of International Council of the Aeronautical Sciences, September 13-18, Melbourne, Australia, pp. 13-20.

Benhamza A, Boubekri A, Atia A, Hadibi T, Arıcı M. 2021. Drying uniformity analysis of an indirect solar dryer based on computational fluid dynamics and image processing. Sustain Energy Techn Asses, 47: 101466.

Bulut S, Unveren M, Arisoy A, Boke Y. 2011. Reducing internal losses in air handling units with CFD analysis method. TMMOB X. National Plumbing Engineering Congress and Exhibition, İzmir, Türkiye, pp: 291-326.

Chen YS, Kim SW. 1987. Computation of turbulent flows using an extended k-epsilon turbulence closure model. URL: https://ntrs.nasa.gov/citations/19880002587 (accessed date: January 15, 2023).

Erdoğan A, Taçgün E, Canbazoğlu S, Aksoy İ G, Kaya A, Sönmez K, Kamer M S, Şahin H E. 2016. A numerical investigation on pressure loss in a chamber with truncated pyramid perforated diffuser designed for air handling units. 8th International Ege Energy Symposium and Exhibition, May 11-13, Afyon, Türkiye, pp. 823-828.

Erdoğan A. 2017. Investigation of airflow in empty chambers with perforated diffuser designed for air handling units in terms of flow and acoustic. PhD Thesis, İnönü University, Institute of Science, Malatya, Türkiye, pp: 115.

Fluent A. 2009. 12.0 User's guide. Ansys inc, 6, 552.

Gan G, Riffat SB. 1997. Pressure loss characteristics of orifice and perforated plates. Experim Thermal Fluid Sci, 14(2): 160-

165.

Gaulke D, Dreyer ME. 2015. CFD simulation of capillary transport of liquid between parallel perforated plates using Flow3D. Micrograv Sci Tech, 27: 261-271.

Gessner F, Jones J. 1965. On some aspects of fully-developed turbulent flow in rectangular channels. J Fluid Mechan, 23(4): 689-713.

Guo B, Hou Q, Yu A, Li L, Guo J. 2013. Numerical modelling of the gas flow through perforated plates. Chem Eng Res Design, 91(3): 403-408.

He Y, Liu XH, Zhang HL, Zheng W, Zhao FY, Schnabel MA, Mei Y. 2021. Hybrid framework for rapid evaluation of wind environment around buildings through parametric design, CFD simulation, image processing and machine learning. Sustain Cities Soc, 73: 103092.

Hu HH. 2012. Computational fluid dynamics. Elsevier, New York, US, pp: 421-472.

Hussain A, Reynolds W. 1975. Measurements in fully developed turbulent channel flow. J Fluids Eng, 1975: 568-578.

Kamer M, Erdoğan A, Tacgun E, Sonmez K, Kaya A, Aksoy I, Canbazoglu S. 2018. A performance analysis on pressure loss and airflow diffusion in a chamber with perforated V-profile diffuser designed for air handling units (AHUs). J Appl Fluid Mechan, 11(4): 1089-1100.

Li J, Agarwal RK, Zhou L, Yang B. 2019. Investigation of a bubbling fluidized bed methanation reactor by using CFD-DEM and approximate image processing method. Chem Eng Sci, 207: 1107-1120.

Özahi E. 2015. An analysis on the pressure loss through perforated plates at moderate Reynolds numbers in turbulent flow regime. Flow Measur Instrumentat, 43: 6-13.

Parsons RA. 1996. 1996 Ashrae Handbook Heating, Ventilating, and Air-Conditioning Systems and Equipment: Inch-Pound Edition. ASHARE, Atlanta, US, pp: 667.

Sönmez K, Özmen Y. 2022. Numerical investigation of the effects of plate diffusers in central air handling units on flow field and pressure drop. Eng Machin, 63(707): 333-358.

Sönmez K. 2017. A numerical investigation of the effect of diffusion flow and pressure reduction of perforeted cutting cone profile diffuser designed for empty cells in air handling units. MSc Thesis, Kahramanmaraş Sütçü İmam University, Institute of Science, Kahramanmaraş, Türkiye, pp: 68.

Tu J, Yeoh GH, Liu C, Tao Y. 2023. Computational fluid dynamics: a practical approach. Elsevier, Heinemann, Germany, pp: 477.

Vakkasoglu AV, Kamer MS, Kaya A. 2021. The effect of different diffusers designed for empty cells in central air handling units on flow and pressure drop. Sci Tech Built Environ, 27(1): 28-43.

Versteeg HK, Malalasekera W. 2007. An introduction to computational fluid dynamics: the finite volume method. Pearson Education.

Wang P, Pan W, Dai G. 2020. A CFD-based design scheme for the perforated distributor with the control of radial flow. AIChE J, 66(5): e16901.

Xu Z, Gotham D, Collins M, Coney J, Sheppard C, Merdjani S. 1996. CFD prediction of turbulent recirculating flow in an industrial packaged air-conditioning unit. HVAC&R Res, 2(3): 195-213.